

Estimating the Competitive Storage Model: A Simulated Likelihood Approach*

Tore Selland Kleppe[†] Atle Oglend[‡]

January 10, 2017

Abstract

This paper develops a particle filter maximum likelihood estimator for the competitive storage model. The estimator is suitable for inference problems in commodity markets where only reliable price data is available for estimation, and shocks are temporally dependent. The estimator efficiently utilizes the information present in the conditional distribution of prices when shocks are not iid. Compared to Deaton and Laroque's composite quasi-maximum likelihood estimator, simulation experiments and real-data estimation show substantial improvements in both bias and precision. Simulation experiments also show that the precision of the particle filter estimator improves faster than for composite quasi-maximum likelihood with more price data. To demonstrate the estimator and its relevance to actual data, we fit the storage model to data set of monthly natural gas prices. It is shown that the storage model estimated with the particle filter estimator beats, in terms of log-likelihood, commonly used reduced form time-series models such as the linear AR(1), AR(1)-GARCH(1,1) and Markov Switching AR(1) models for this data set.

Keywords: commodity prices, competitive storage model, particle filter, rational expectations, simulated likelihood

JEL codes: C13, C15, D22

*The authors are indebted to the Editor; Ana Colubi, two anonymous reviewers, Frank Asche, Hans Karlsen, Hans Julius Skaug and Bård Støve for comments that greatly improved the paper.

[†]University of Stavanger, Department of Mathematics and Natural Sciences (Corresponding author: email: tore.kleppe@uis.no, address: University of Stavanger, 4036 Stavanger, Norway, telephone: +47 51831717, fax: +47 51831750)

[‡]University of Stavanger, Department of Industrial Economics

1 Introduction

This paper addresses the problem of estimating the structural parameters of the competitive storage model when only price data is available for estimation and supply shocks are temporally dependent. We propose and investigate a particle filter estimator based on recently developed methods in the particle filter literature (Gordon et al., 1993; Fernandez-Villaverde and Rubio-Ramirez, 2007; Malik and Pitt, 2011; DeJong et al., 2013). We demonstrate that this estimator has superior large sample properties and improved parameter identification properties over the conventional composite pseudo maximum likelihood estimator (CML) (Deaton and Laroque, 1995, 1996). Compared to the CML, the estimator also displays substantial reduction in bias when it comes to various predicted price characteristics, including price autocorrelation, where the CML estimator appears to underestimate price persistence.

Particle filter methods are suitable to address inference problems in non-linear models with latent variables, and appear especially relevant for low dimensional models such as the partial equilibrium competitive storage model in this paper. Our proposed estimator has the added benefit of being an extension of the CML approach. The CML estimator utilizes invariant distributions to integrate out the latent state variable, in this case the supply shock. This procedure neglects important information present in the conditional price distribution when shocks are temporally dependent. It is this information the particle filter estimator makes use of when inferring structural parameters.

Improving structural model estimates provides better comparison between competing commodity price models. We apply our estimator to a natural gas price data set, and compare the structural model to popular reduced form models such as the linear AR(1) model, AR(1)-GARCH(1,1) model and a Markov Switching AR(1) model. The comparison to reduced form models allows identification of what price features the storage model is able to account for, and where improvements are needed. For the natural gas market, the storage model performs better than all the reduced form time-series models considered, in terms of log-likelihood. This suggests that the non-linearity in the model, arising from the non-negativity constraint on storage, is relevant for natural gas price characteristics. As support for the relevance of the storage model for natural gas we also find a relatively strong correspondence between observed and model implied storage. The overall diagnostics show that the storage model addresses features in the higher moments of prices, specifically linked to excess kurtosis and ARCH effects.

The competitive storage model is the prevailing economic model explaining price dynamics of storable commodities. The model incorporates effects of speculative storage behavior on market dynamics in a rational expectations framework. The model in its current form can trace its origins to the Theory of Storage (Williams, 1936; Kaldor, 1939; Working, 1949). Since the storage model explicitly recognizes the role of

profit maximizing storage behavior, it is often used to examine implications of different commodity market policies and regulations. Miranda and Helmberger (1988) used the storage model to investigate the effects of government price support programs in the U.S. soybean market. Gouel (2013b) analyzed various food price stabilization policies (public stocks, state contingent subsidy/tax on production) using an extension of the competitive storage model with risk averse consumers and incomplete insurance markets. Similarly, Brennan (2003) used the storage model to analyze the effects of public interventions in the Bangladesh rice market. Meaningful policy evaluations using structural models require suitable model parameters.

The theoretical foundation of the model is well established by now. What has proved more difficult is confronting the model with data in order to operationalize it for practical policy analysis and hypothesis testing. Estimation has been limited by two factors: (1) the lack of a closed form solution to the model, necessitating a computationally demanding subroutine to solve a dynamic optimization problem for each parameter evaluation, and (2) lack of reliable quantity data. With improved computational power the first factor is becoming less important, although the curse of dimensionality quickly rebalances growth in computational power. For data availability, some commodity markets do have reliable quantity data. The London Metal Exchange (LME), for instance, provides information on metal stocks in LME warehouses (see Geman and Smith (2013) for an analysis of the Theory of Storage as applied to the LME metals). Miranda and Glauber (1993) estimate the storage model using stock and price data from the U.S. soybean market. Price data however remains the most accessible, and arguably highest quality, commodity data. Because of this, price data should in general be used when estimating the storage model. We provide simulation evidence which shows that price data is sufficient to fully identify the structural parameters of the model when the particle filter estimator is applied, even when shocks are not iid. For model verification and hypothesis testing it is also desirable to retain some data to test model predictions. We illustrate this in the empirical application part of the paper when we compare model implied storage, derived using only price data, with actual storage.

An early step towards empirical testing of the model can be found in Wright and Williams (1982). The authors provide numerical solutions to the model under different specifications, and confirm that model implied behavior is consistent with observations of some important commodities. One important feature of the storage model is the non-negativity constraint on storage. This constraint makes the model non-linear; the no-arbitrage restriction characterizing profit maximizing storage can fail if the commodity is sufficiently scarce. Prices will move between two pricing regimes defined by whether or not the no-arbitrage restriction holds. Which regime is active depends on current price relative to a threshold price marking the cut-off point where the no-arbitrage restriction fails. Deaton and Laroque (1992) and Ng (1996) estimate threshold prices for various commodities using a generalized method of moments estimator and find evidence for regime behavior consistent with model predictions.

Full structural estimation without quantity data was achieved in a series of pioneering papers by Deaton and Laroque (1992, 1995, 1996). Deaton and Laroque estimated the model on price data by means of a composite pseudo maximum likelihood estimator. Although a significant step forward, the efficiency and precision of the estimator has been questioned. Michaelides and Ng (2000) show, using Monte Carlo simulations, that the CML estimator tends to bias the estimates. The authors also find that none of the simulation estimators beat the CML estimator in a mean-squared sense, but that they have improved bias properties. The particle filter estimator in this paper addresses the CML estimator bias. Cafiero et al. (2006) argue that the crucial kink in the pricing function, due to the non-negativity constraint on storage, is imprecisely estimated because of the smoothing effects of spline methods used to interpolate between grid points. Cafiero et al. (2011) show that precision can be greatly improved by increasing the number of grid points used to approximate the pricing function. Recently Cafiero et al. (2015) proposed a maximum likelihood estimator of the storage model with small properties superior to that of the pseudo maximum likelihood approach. Their estimator relies of iid normal supply shocks, and as such does not allow for temporal shock dependence. The estimator considered in this paper provides an alternative to the maximum likelihood estimator of Cafiero et al. (2015) in the case of temporal shock dependence.

By allowing for shock dependence, our paper deviates somewhat from the empirical literature on the model. With the exception of Deaton and Laroque (1995, 1996), most applications assume iid shocks. One problem iid shocks is that predicted price persistence is lower than what is typically observed. This can be partly remedied by increasing the number of grid points used to approximate the pricing function (Cafiero et al., 2011). Extensions to the basic model such as allowing for an explicit convenience yield component (Miranda and Rui, 1996; Ng and Ruge-Murcia, 2000), gestation lags in production (Ng and Ruge-Murcia, 2000), the effect of news on future production (Osborne, 2004) and storage frictions (Mitraille and Thille, 2009) have also been shown to increase model price autocorrelation. The basic model has also been extended to a more general equilibrium framework (Funke et al., 2011; Arseneau and Leduc, 2013), and to consider monopolistic behavior in speculative storage (Mitraille and Thille, 2009). Temporal dependence in supply and/or demand shocks is not unreasonable for the types of partial equilibrium models that the basic competitive storage model represents. Any non-modeled stochastic exogenous effects must enter through the specified shock processes. Slowly changing macroeconomic conditions, for instance, is likely to give rise to persistence in demand for the commodity. Overall, it seems unreasonable to expect that speculative storage alone can fully account for the substantial shock persistence observed in commodity prices. In the additive, single shock, formulation of the standard competitive storage model, positive demand shocks are equivalent to negative supply shocks, and supply shocks should be interpreted as net-supply shocks.

Another issue in the Deaton and Laroque CML estimation is the use of observed Fisher information to

derive asymptotic standard deviations of estimated parameters. However, we have found that asymptotic results can be misleading for sample sizes relevant to this methodology. To work around this complication, we make no effort to make the log-likelihood smooth. Rather we introduce a full parametric specification consistent with the moments of the storage model and rely on parametric bootstrap for estimating statistical standard errors. The validity of the parametric specification is then tested via generalized residuals.

The paper proceeds as follows. In section 2 we give a description of the storage model. Section 3 describes the estimation methodology. Following this we investigate the performance of the estimator on simulated data in section 4. Comparing the estimator to the CML estimator we find that bias is substantially reduced. In addition the precision of key structural parameters are greatly improved. In section 5 we apply the estimation procedure to a natural gas data set and find evidence that the non-negativity constraint on storage is relevant in describing key properties of prices. Finally, section 6 concludes.

2 The Storage Model

Before turning to the issue of estimating structural parameters, we provide a brief description of the basic competitive storage model with autocorrelated supply shocks. The model is the same as in Deaton and Laroque (1995, 1996), from now on referred to as DL. For more details on the model see Deaton and Laroque (1996).

Assume at any time there is exogenous stochastic supply z_t , which follows a first-order linear autoregressive process: $z_t = \rho z_{t-1} + \epsilon_t$, where ϵ_t is a standard normal random variable. The supply shock is what fundamentally drives variations in prices. The market consists of consumers and risk-neutral competitive speculators that hold inventories. Following DL, we assume a proportional decay of stocks in storage. The constant depreciation rate δ accounts for the direct cost of storage, and is a structural parameter to be estimated. Let I_t be the level of inventories at time t . The amount of stocks on hand x_t and supply z_t then follow the laws of motion:

$$x_t = (1 - \delta) I_{t-1} + z_t, \tag{1}$$

$$z_t = \rho z_{t-1} + \epsilon_t. \tag{2}$$

The problem facing speculators is choosing the level of inventories to maximize the expected discounted profits from storage. In this paper, as in DL, consumers are assumed to hold linear inverse demand, represented by $P(z) = a + bz$, where a and $b < 0$ are structural parameters. The opportunity cost of capital tied

to storage is assumed a fixed real interest rate r per period. Combined with the depreciation rate, $\beta = \frac{1-\delta}{1+r}$ accounts for the cost of storing one unit of the commodity for one period. There are two state variables relevant to the optimal storage decision at any time, the current stock level x_t and the current state of the supply shock z_t . Let $V(x_t, z_t)$ be the value of the commodity stock at time t given competitive speculators follow an optimal storage policy. This value function must satisfy the Bellman functional equation

$$V(x_t, z_t) = \max_{I_t} \{p_t(x_t - I_t) + \beta E_t V((1 - \delta)I_t + z_{t+1}, \rho z_t + \epsilon_{t+1})\}, \quad (3)$$

where the maximization is subject to equations (1),(2) and the non-negativity constraint $I_t \geq 0$. Note that $x_t - I_t$ is the amount supplied to the market, and p_t the commodity price at time t . The price is considered fixed when making storage decisions and speculators are assumed to hold rational expectations. Given storage is not bounded, $I_t > 0$, profit maximizing competitive storage implies the no-arbitrage restriction: $\beta E_t p_{t+1} = p_t$ (this follows from taking the derivative of equation 3 w.r.t. to I_t , setting equal to zero, and applying the envelope theorem). The no-arbitrage relationship will fail if $P(x_t) \geq \beta E_t p_{t+1}$, in which case optimal storage must be $I_t = 0$ (stock-out). The optimal storage policy implies the following restriction:

$$p_t = \max [P(x_t), \beta E_t p_{t+1}] \quad (4)$$

The restriction states that if selling the entire stock x_t gives a higher price than what could be gained from storing, zero storage is optimal and current price is dictated by consumer willingness to pay for existing stocks, $P(x_t)$. Otherwise, the no-arbitrage condition holds and profit maximizing storage ensures current price p_t equal to $\beta E_t p_{t+1}$.

Provided supply has compact support and inventories are costly $\beta < 1$, Deaton and Laroque (1992) and Chambers and Bailey (1996) prove that a solution to (4) exist in the form of a rational expectations pricing function $p = f(x, z)$. The pricing function $f(x, z)$ gives the competitive equilibrium price p consistent with optimal storage at states x and z and market clearing. The function in general has no closed form solution and must be solved for numerically. The mapping $p = f(x, z)$ is the solution to the functional equation:

$$f(x, z) = \max \left[\beta \int f(\epsilon + \rho z + (1 - \delta)(x - P^{-1}(f(x, z))), \epsilon + \rho z) d\Phi(\epsilon), P(x) \right] \quad (5)$$

where $\Phi(\epsilon)$ is the standard normal distribution function. For given parameters, the function can be found by conventional numerical procedures, we refer to section 3.1 for the specific numerical procedure used in this paper. The price function provides the means to generating the predictive moments necessary for estimation purposes.

3 Estimation Methodology

The problem at hand is to estimate the structural parameters: $\theta = [\rho, a, b, \delta]$. By utilizing the price function (5) we can construct the one-period ahead mean and variance of price as a function of current price p_t and supply shock z_t . We define these quantities respectively as $\mu(p_t, z_t) := E(p_{t+1}|p_t, z_t)$ and $\sigma^2(p_t, z_t) := Var(p_{t+1}|p_t, z_t)$. This procedure allows the construction of the likelihood over all observed prices. For the model with autocorrelated shocks, the conditional mean and variance depend on the unobserved supply shock z_t . As such z_t must be integrated out of the conditional moments. To achieve this, DL integrate over the invariant distributions of z_t conditionally on p_t . However, using invariant distributions do not utilize the full information available from the observables about the state of the system, and is likely to be inefficient, as was recognized by DL themselves. Simulation evidence provided below also suggest that the invariant distribution integration does not lead to improved large sample properties of the estimator; the bias of the estimates does not appear to shrink as more price data becomes available. In the following we propose a particle filter approach to deal with this problem. The particle filter avoids using invariant distributions, which provides more efficient and precise estimates.

Throughout we let $\mathcal{N}(x; \mu, \sigma^2)$ denote the $N(\mu, \sigma^2)$ density evaluated at x . Moreover, for consistency with the notation of DL who already use p and f , we use $\pi(x)$ as the generic symbol for probability density functions.

3.1 Numerical solution of the price function equation

As for most non-linear rational expectation models, obtaining a closed form solution to the dynamic optimization problem characterized by (5) is not possible, and we must resort to numerical methods. A large body of literature, surveyed in e.g. Miranda (1997); Aruoba et al. (2006); Gouel (2013a), is devoted to such numerical solutions. The price function $f(x, z)$ is known to have discontinuous derivatives w.r.t. x at the point $x^*(z)$, the threshold stock level where the no-arbitrage restriction breaks down for stocks below this level, i.e. where $I = 0$ for $x \leq x^*(z)$. The threshold stock level is characterized by

$$x^*(z) = \sup\{x; f(x, z) = P(x)\}.$$

To solve for the price function $f(x, z)$ we iterate on the recursive formulation of equation 5. This provides a quick and reliable numerical approximation to $f(x, z)$. Perturbation- and spectral methods appear less applicable for non-smooth solutions, and are also in general more time consuming. Our implementation is similar in spirit to that of DL, but differs in particular in the choices of grids.

3.1.1 Price function iteration grid

When choosing the grid over which the price function is computed, several aspects have to be taken into consideration. Firstly, the grid has to be fine enough to avoid substantial biases in the parameter estimates (Cafiero et al., 2011). Moreover, since the price function is computed for many sets of parameters during the numerical maximization of the likelihood, computational tractability must be kept in mind. Finally, the price function must be continuous w.r.t. the parameters, and therefore rules out any adaptive strategies for finding grids.

The specific grids employed are in the z -direction (supply shocks) equally spaced with M_z grid-points Z_1, \dots, Z_{M_z} . Throughout most of this work, M_z is set to 64. The grid is chosen to cover 6 standard deviations of the unconditional distribution of z_t , corresponding to $Z_1 = -6/\sqrt{1-\rho^2}$ and $Z_{M_z} = 6/\sqrt{1-\rho^2}$. Compared to DL, who used 11 grid points and a discretization similar to that of Tauchen (1986), our grid is more finely spaced and covers a larger range. This reflect both access to faster- and parallel computing and the fact that the later described particle filter sometimes request evaluations of $z \mapsto f(x, z)$ in areas that are very unlikely to be visited under the marginal distribution of z_t .

In the x -direction (stocks), we divide the grid over which $f(x, z)$ is computed into two parts. First, a finer equally spaced grid with $M_{x,1}$ grid points covering the lower range of x known to contain $x^*(z)$ for all relevant values of z . Second, a coarser equally spaced grid with $M_{x,2}$ grid points covering the higher range of x where $x \mapsto f(x, z)$ is slowly varying. The grid points are denoted by $X_1, \dots, X_{M_{x,1}+M_{x,2}}$, and for most of this work, $M_{x,1} = M_{x,2} = 128$. The range of the first grid is set to

$$X_1 = \min(P^{-1}(p_{max}), Z_1), X_{M_{x,1}} = \max\left(-\frac{a}{b}, Z_{M_z}\right).$$

where p_{max} is larger than the observed maximum price¹. In the definition of X_1 , $P^{-1}(p_{max})$ ensures that the numerical representation of $f(x, z)$ spans sufficiently high prices, and Z_1 reflects that stock at hand cannot be smaller than the smallest supply (Deaton and Laroque, 1996). In the upper limit of the first grid, $-a/b$ ensures that $X_{M_{x,1}} \geq x^*(z)$ since $f(-a/b, z) > P(-a/b) = 0$. Moreover, Z_{M_z} is chosen less rigorously based on experience to ensure numerical accuracy in cases when the demand slope b is large in magnitude. The second grid is uniformly spaced with

$$X_{M_{x,1}+1} = X_{M_{x,1}} + (X_{M_{x,1}+M_{x,2}} - X_{M_{x,1}})/M_{x,2}, X_{M_{x,1}+M_{x,2}} = cZ_{M_z}/\delta.$$

The upper x -range of the grid is inspired by DL, who obtain that the stock at hand x_t asymptotes to Z_{M_z}/δ

¹In this work we typically set $p_{max} = 20$ as the real data sets are normalized to have unit mean.

when the supply is always at maximum Z_{M_z} and no stock is consumed. However, we have included the factor $c = 1.5$ obtained by trial and error to ensure that sufficiently low prices are always represented, in particular when the numerical optimizer tries values of the parameters that are inconsistent with the data at hand.

3.1.2 Price function iteration

Equation (5) defines a functional fixed point for $f(x, z)$ which we iterate from an initial guess. Our numerical solution, say $\hat{f}(x, z)$, obtains as a bilinear interpolation between tabulated values over the previously discussed grid. The integral in (5) for each grid point (X_i, Z_j) is approximated as

$$\int f(\epsilon + \rho Z_j + (1 - \delta)(X_i - P^{-1}(f(X_i, Z_j))), \epsilon + \rho Z_j) d\Phi(\epsilon), \quad (6)$$

$$\approx \int \hat{f}(\eta + (1 - \delta)(X_i - P^{-1}(\hat{f}(X_i, Z_j))), \eta) \mathcal{N}(\eta; \rho Z_j, 1) d\eta, \quad (7)$$

$$\approx \sum_{k=1}^{M_z} \hat{f}(Z_k + (1 - \delta)(X_i - P^{-1}(\hat{f}(X_i, Z_j))), Z_k) W_{j,k}, \quad (8)$$

where the weight matrix W has elements

$$W_{j,k} = \frac{\mathcal{N}(Z_k; \rho Z_j, 1)}{\sum_{l=1}^{M_z} \mathcal{N}(Z_l; \rho Z_j, 1)}, \quad j, k = 1, \dots, M_z.$$

I.e. each row in the weight matrix represents discrete distribution over $\{Z_1, \dots, Z_{M_z}\}$ having probability masses proportional to $\mathcal{N}(Z_k; \rho Z_j, 1)$, $k = 1, \dots, M_z$. The reason for choosing this particular discretization follows the insight of DL that it leads to $\hat{f}(x, z)$ being evaluated only at grid points in the z -direction. Thus the evaluation of each term in the sum (8) is reduced to a univariate linear interpolation problem in the x -direction.

Equipped with the integral approximation (6 - 8), the price function iteration is started at $\hat{f}(x, z) = \max(P(x), 0)$, and proceeds by alternating between

$$\begin{aligned} G(X_i, Z_j) &= \beta \sum_{k=1}^{M_z} \hat{f}(Z_k + (1 - \delta)(X_i - P^{-1}(\hat{f}(X_i, Z_j))), Z_k) W_{j,k}, \\ \hat{f}(X_i, Z_j) &= \max(P(X_i), G(X_i, Z_j)), \end{aligned}$$

for $i = 1, \dots, M_{x,1} + M_{x,2}$, $j = 1, \dots, M_z$. Throughout this work, we perform 400 iterations, as a fixed number of iterations are required to obtain a continuous likelihood. This number of iterations is typically sufficient to bring maximal absolute change in \hat{f} at the last iteration to $\sim 1e - 3$. The outer loop over i is performed in parallel over 8 kernels on the computer applied and the overall routine for calculating \hat{f} requires ~ 1 second when implemented in Fortran 90.

3.1.3 Predictive moments

The predictive moments $\mu(p_t, z_t) = E(p_{t+1}|p_t, z_t)$ and $\sigma^2(p_t, z_t) = \text{Var}(p_{t+1}|p_t, z_t)$ are required to form the likelihood function of the data. We compute them in two steps. First, the time t stock at hand $x_t = x_t(p_t, z_t)$ is recovered, modulo price function approximation error, from p_t and z_t by solving $p_t = \hat{f}(x_t, z_t)$ for x_t . In practice, this is implemented using a binary search in the x -direction. As bilinear interpolation is employed to compute $\hat{f}(x, z)$ off the grid, we have not encountered cases where $x \mapsto \hat{f}(x, z)$ is not monotone, and therefore no problems with non-uniqueness of x_t was encountered.

Secondly, the predictive mean is calculated using that

$$\begin{aligned} \mu(p_t, z_t) &= E(p_{t+1}|p_t, z_t) = E(f(x_{t+1}, z_{t+1})|p_t, z_t) \\ &= E(f((1-\delta)I_t + z_{t+1}, z_{t+1})|p_t, z_t), \\ &= \int f((1-\delta)[x_t(p_t, z_t) - P^{-1}(p_t)] + \rho z_t + \epsilon_{t+1}, \rho z_t + \epsilon_{t+1}) d\Phi(\epsilon_{t+1}), \end{aligned}$$

and a completely analogous argument applies for the conditional variance $\sigma^2(p_t, z_t)$. Storage I_t is here derived as the difference between implied stock $x_t(p_t, z_t)$ and consumption $P^{-1}(p_t)$. In practice, we implement these integrals using 16-point Gauss-Hermite quadrature and substituting \hat{f} for f .

3.2 Inference

In their inference, DL do not specify a parametric family for $p_{t+1}|p_t, z_t$, and use quasi maximum likelihood² for estimation. Here we depart in taking $p_{t+1}|p_t, z_t$ to be Gaussian to obtain a, conditionally on p_1 , complete parametric model

$$p_{t+1} = \mu(p_t, z_t) + \sqrt{\sigma^2(p_t, z_t)}\eta_{t+1}, \quad \eta_t \sim \text{i.i.d. } N(0, 1), \quad t = 1, \dots, T-1, \quad (9)$$

$$z_{t+1} = \rho z_t + \epsilon_{t+1}, \quad \epsilon_t \sim \text{i.i.d. } N(0, 1), \quad t = 1, \dots, T-1, \quad (10)$$

$$z_1 \sim N\left(0, \frac{1}{1-\rho^2}\right), \quad (11)$$

that is consistent with the moments of the price process of the storage model. It is worth noticing that $p_{t+1}|p_t, z_t \sim N(\mu(p_t, z_t), \sigma^2(p_t, z_t))$ does not imply that $p_{t+1}|p_t$ or $p_{t+1}|p_1, \dots, p_t$ are Gaussian. Rather, the unconditional transition laws are complicated mean-variance mixtures of Gaussians that can exhibit skewness and heavy tails.

The reason for choosing a parametric model is mainly for convenience, as doing so grants us access to

² In the sense of substituting unspecified families of distributions with Gaussians (Gourieroux et al., 1984).

the likelihood analysis toolbox and parametric bootstrapping. Moreover, the diagnostics reported later allow us to test whether imposing a Gaussian distribution on η_t is reasonable. Quasi maximum likelihood, on the other hand, would be complicated due to the lack of reliable derivatives to form sandwich formulas, and is not easily bootstrapped.

The model (9-11) is, for observations p_1, \dots, p_T , a dynamic latent variable model, with dependence structure typical of a time-discretized diffusion model, and the conditional likelihood function is expressed in terms of

$$L(\theta|p_1, \dots, p_T) = \pi(p_2, \dots, p_T|p_1) = \int \pi(z_1) \prod_{t=2}^T \pi(p_t, z_t|p_{t-1}, z_{t-1}) dz_1 \cdots dz_T. \quad (12)$$

To circumvent integrating over z_t , DL uses a composite likelihood technique (Lindsay, 1988) where the product of likelihoods of consecutive pairs of prices is substituted for the full likelihood. Using composite likelihoods is known to result in loss of estimation efficiency (Varin and Vidoni, 2008) over full likelihood-based techniques as we propose here. A large body of literature is devoted to fully likelihood-based inference in models with this structure, and include Bayesian Markov chain Monte Carlo (MCMC) (Eraker, 2001) and simulated maximum likelihood (Durbin and Koopman, 1997; Shephard and Pitt, 1997; Durham, 2006). As the calculation of \hat{f} for each combination of the parameters is expensive, MCMC (including the particle MCMC approach of Andrieu et al. (2010); Pitt et al. (2012)) would be very time consuming. Moreover, the fact that $z_t \mapsto \log \pi(p_{t+1}|p_t, z_t)$, implied by (9), is a non-smooth function bars the usage of smoothing-based importance samplers such as Durbin and Koopman (1997); Shephard and Pitt (1997); Liesenfeld and Richard (2003); Richard and Zhang (2007). Consequently, we resort to simulated maximum likelihood, where the likelihood function is calculated using a continuous particle filter in the spirit of Malik and Pitt (2011) to obtain efficient estimators and retain computational tractability.

3.2.1 Simulated likelihood

To estimate the marginal log-likelihood $l(\theta) = \log L(\theta|p_1, \dots, p_T)$ at a fixed parameter θ , we take as vantage point the sampling importance resampling (SIR) particle filter (Gordon et al., 1993), adapted to time-discretized diffusion structures as described in Durham (2006). The filter with N particles may be described as follows:

1. Initialization: set $t = 1$, $\hat{l} = 0$
2. Simulate $z_{t,pred}^{(j)} \sim \pi(z_1)$, $j = 1, \dots, N$.
3. Compute $w_t^{(j)} = \pi(p_{t+1}|p_t, z_{t,pred}^{(j)})$ and set $L_t = \frac{1}{N} \sum w_t^{(j)}$. [L_t is an approximation to $\pi(p_{t+1}|p_1, \dots, p_t)$]
4. Set $\hat{l} \leftarrow \hat{l} + \log(L_t)$. [\hat{l} is an approximation to $\log \pi(p_2, \dots, p_{t+1}|p_1)$]

5. Re-sample N particles from $z_{t,pred}^{(j)}$ with weights $w_t^{(j),*} = w_t^{(j)} / \sum_{k=1}^N w_t^{(k)}$ to form $z_{t,fill}^{(j)}$, $j = 1, \dots, N$. $\left\{ z_{t,fill}^{(j)} \right\}_{j=1}^N$ is an equally weighted representation of $\pi(z_t | p_1, \dots, p_{t+1})$
6. Simulate $z_{t+1,pred}^{(j)} \sim \pi(z_{t+1} | z_t = z_{t,fill}^{(j)})$, $j = 1, \dots, N$. $\left\{ z_{t+1,pred}^{(j)} \right\}_{j=1}^N$ is an equally weighted representation of $\pi(z_{t+1} | p_1, \dots, p_{t+1})$
7. If $t < T - 1$, set $t \leftarrow t + 1$ and go to step 3.

It is well known (see e.g. Malik and Pitt, 2011) that the resampling in step 5 originate discontinuous likelihood approximations even if the same random numbers are used for repeated evaluation of $\hat{l}(\theta)$ for different values of the parameters, and thereby renders subsequent numerical maximization difficult. Malik and Pitt (2011) propose to obtain draws in step 5 based on a smoothed version of the empirical distribution function of the weighted sample $(z_{t,pred}^{(j)}, w_t^{(j),*})$. We follow a different path to obtain a continuous likelihood, in combining step 5 and 6. Write

$$\pi(z_t | p_1, \dots, p_{t+1}) \approx \sum_{j=1}^N w_t^{(j),*} \delta(z_t - z_{t,pred}^{(j)})$$

where $\delta(\cdot)$ denotes a unit point mass in 0. Then

$$\pi(z_{t+1} | p_1, \dots, p_{t+1}) \approx \sum_{j=1}^N w_t^{(j),*} \mathcal{N}(z_{t+1} | \rho z_{t,pred}^{(j)}, 1)$$

which can be sampled from continuously using inversion sampling. We use a fast Fourier transform method (Kleppe and Skaug, 2016) based on stratified uniform common numbers described in Appendix A which has the same computational complexity of $O(N \log_2(N))$ as the method of Malik and Pitt (2011). Notice that advancing to the supply process (step 6) does not involve simulation, which will have desirable effect on Monte Carlo variability of overall Monte Carlo estimate of the log likelihood $\hat{l}(\theta)$.

A number of improved particle filters have been proposed in literature (see Cappe et al., 2007, for a survey) with the prospect of further reducing Monte Carlo variation. However, for relevant ranges of the parameters, the model (9-11) has a low signal-to-noise ratio. Thus does our simple modified SIR filter produce sufficiently precise estimates of the log-likelihood for moderate N . E.g. for $T \sim 1000$, $N = 4096$ and the filter implemented in Fortran 90 produces acceptable accuracy while the computing times of an evaluation of $\hat{l}(\theta)$ is on the same order as the time required to compute \hat{f} .

3.2.2 Algorithm, estimation and standard errors

Based on the above introduced notation, to evaluate $\hat{l}(\theta)$ for any given θ and price series p_1, \dots, p_T requires the following steps:

1. Solve numerically the price function $\hat{f}(x, z)$ as described in section 3.1-3.1.2 for parameter θ .
2. Set $t = 1$, $\hat{l} = 0$ and simulate $z_t^{(j)} \sim N(0, 1/(1 - \rho^2))$, $j = 1, \dots, N$.
3. Compute $\mu(p_t, z_t^{(j)})$, $\sigma^2(p_t, z_t^{(j)})$ for $j = 1, \dots, N$ based on the numerical solution of the price function as described in Section 3.1.3 and set $w_t^{(j)} = \mathcal{N}(p_{t+1} | \mu(p_t, z_t^{(j)}), \sigma^2(p_t, z_t^{(j)}))$, $w_t^{(j),*} = w_t^{(j)} / \sum_{k=1}^N w_t^{(k)}$ for $j = 1, \dots, N$.
4. Set $L_t = \frac{1}{N} \sum w_t^{(j)}$ and $\hat{l} \leftarrow \hat{l} + \log(L_t)$.
5. Simulate $z_{t+1}^{(j)} \sim \sum_{k=1}^N w_t^{(k),*} \mathcal{N}(z_{t+1} | \rho z_t^{(k)}, 1)$, $j = 1, \dots, N$ using the FFT-based method described in Appendix A.
6. If $t < T - 1$, set $t \leftarrow t + 1$ and go to step 3. Otherwise return $\hat{l}(\theta) = \hat{l}$.

The use of bilinear interpolation for evaluation of \hat{f} off the grid results in $\hat{l}(\theta)$ having discontinuous derivatives. Thus gradient-based optimizers are not suitable, and we therefore find the simulated maximum likelihood estimator $\hat{\theta} = \arg \max \hat{l}(\theta)$ using the Nelder-Mead type optimizer implemented in MATLAB's `fminsearch` routine.

The lack of continuous derivatives also bars estimating reliable parameter standard errors using the observed Fisher information matrix. Instead, we rely on parametric bootstrap, where the simulated maximum likelihood estimator is applied to synthetic data simulated from the model (9-11).

3.2.3 Properties of the simulated maximum likelihood estimator

All structural parameters in the model are statistically identified given the non-negativity constraint on storage is not at all times binding. The price process implied by the model moves between two regimes dependent on the storage constraint. The only parameter unique to the positive storage regime is depreciation δ . As this tends to one, storage becomes increasingly costly and the storage regime less relevant. We show in the empirical application below that under zero speculative storage, the price process reduces to a linear AR(1) process, which is stationary and mean reverting given the supply shock is stationary and mean reverting. At the other extreme, where depreciation tends to $-r$, storage becomes costless and the storage constraint less likely to be binding. The parameters will still be identified, but the non-linearity arising from the regime-shifts will be less relevant to the price dynamics. Indeed, the primary feature of the DL formulation of the storage model is that the market should move between regimes where speculative storage occurs and where there is a speculative storage stock-out. The relevance of this regime shift feature can be checked by looking at the probability of model implied stock levels moving below a level where speculative storage is profitable. We do this in our empirical application below.

3.2.4 Diagnostics

When carrying out diagnostics tests on time series models, a standard approach is to carry out a battery of tests on the residuals. For the dynamic latent variable models, calculating and characterizing residuals are complicated by the presence of the latent factor. For model (9-11), both $p_{t+1}|p_t$ and $p_{t+1}|p_1, \dots, p_t$ are complicated non-linear (in p_t or p_1, \dots, p_t) mean-variance mixtures of Gaussians without closed form expressions. Consequently we resort to generalized residuals as explained in Durham (2006). For a correctly specified model, the probability u_t of observing p_t or smaller, conditionally on p_1, \dots, p_{t-1} should be iid uniformly distributed. Fortunately, these generalized residuals u_t can easily be estimated from particle filter output (Durham, 2006) as

$$u_t \approx \hat{u}_t = \frac{1}{N} \sum_{j=1}^N \Phi \left(p_t | \mu(p_{t-1}, z_{t-1}^{(j)}), \sigma^2(p_{t-1}, z_{t-1}^{(j)}) \right), \quad t = 2, \dots, T. \quad (13)$$

Throughout this work, we use for diagnostics purposes the transformed generalized residuals $\hat{\eta}_t = \Phi^{-1}(\hat{u}_t)$, $t = 2, \dots, T$, from now on referred to as the residuals. Under a correctly specified model $\{\hat{\eta}_t\}_{t=2}^T$ should be an iid sequence of standard Gaussian variables. However it is worth noticing that $\{\hat{\eta}_t\}_{t=2}^T$ being Gaussian does not imply that $p_{t+1}|p_1, \dots, p_t$, $t = 1, \dots, T-1$ are Gaussian, only that the distributions of $p_{t+1}|p_1, \dots, p_t$, $t = 1, \dots, T-1$ are correctly captured by the model.

3.3 Composite likelihood estimator

As a benchmark for our proposed simulated maximum likelihood estimator, we also implement a composite quasi maximum likelihood estimator in the spirit of DL. We use the same numerical solution procedure for the price function \hat{f} . This method relies on looking at consecutive pairs of prices (p_t, p_{t+1}) , $t = 1, \dots, T-1$ and finding the unconditional (with respect to z_t) versions of the predictive moments μ , σ^2 as

$$\mu(p_t) = \int \mu(p_t, z_t) \pi(z_t|p_t) dz_t, \quad t = 1, \dots, T-1, \quad (14)$$

$$\sigma^2(p_t) = \int \sigma^2(p_t, z_t) \pi(z_t|p_t) dz_t, \quad t = 1, \dots, T-1, \quad (15)$$

where the conditional $\pi(z_t|p_t)$ derives from the joint stationary distribution $\pi(p_t, z_t)$. For this purpose, DL derive the full joint stationary distribution of (x_t, z_t) on the grid used for solving for f , and thereafter derive distributions of z_t conditional on each observed p_t . In our setup, we advise against this practice, as it involves factorizing a $(M_{x,1} + M_{x,2})M_z \times (M_{x,1} + M_{x,2})M_z = 16384 \times 16384$ unstructured matrix. Instead we rely on a Monte Carlo estimator of $\pi(p_t|z_t)$ which is implemented using the following steps:

1. Simulate a realization $\{(\check{p}_t, \check{z}_t)\}_{t=1}^{n_i n_t}$ of the joint (p_t, z_t) process (9-11) of length $n_i n_t$.
2. Subsample every n_t -th observation of the simulated process to form the less autocorrelated sample $\tilde{S} = \{(\tilde{p}_i, \tilde{z}_i)\}_{i=1}^{n_i}$ where $\tilde{p}_i = \check{p}_{n_t(i-1)+1}$, $\tilde{z}_i = \check{z}_{n_t(i-1)+1}$.
3. Calculate observed mean and variance of \tilde{S} , i.e. $m_p = \frac{1}{n_i} \sum_{i=1}^{n_i} \tilde{p}_i$, $s_p^2 = \frac{1}{n_i-1} \sum_{i=1}^{n_i} (\tilde{p}_i - m_p)^2$, and correspondingly for m_z , s_z^2 .
4. Set up a uniform grid $\underline{Z} = \{z^{(j)}\}_{j=1}^{n_g}$ covering $m_z \pm 4\sqrt{s_z^2}$.

5. For each $t = 1, \dots, T-1$; calculate un-normalized kernel estimate with Gaussian kernels to $\pi(z_t|p_t)$ over \underline{Z} given by

$$\underline{w}_t^{(j)} = \sum_{i=1}^{n_i} \exp\left(-\frac{1}{2} \frac{(p_t - \tilde{p}_i)^2}{h_p^2} - \frac{1}{2} \frac{(z^{(j)} - \tilde{z}_i)^2}{h_z^2}\right).$$

Here the bandwidths are chosen via the simple plug-in rules $h_p = 2n_i^{-\frac{1}{6}} \sqrt{s_p^2}$, $h_z = 2n_i^{-\frac{1}{6}} \sqrt{s_z^2}$.

6. For each $t = 1, \dots, T-1$; approximate (14, 15) as

$$\begin{aligned} \mu(p_t) &\approx \bar{\mu}(p_t) = \frac{\sum_{j=1}^{n_g} \underline{w}_t^{(j)} \mu(p_t, z^{(j)})}{\sum_{j=1}^{n_g} \underline{w}_t^{(j)}}, \\ \sigma^2(p_t) &\approx \bar{\sigma}^2(p_t) = \frac{\sum_{j=1}^{n_g} \underline{w}_t^{(j)} \sigma^2(p_t, z^{(j)})}{\sum_{j=1}^{n_g} \underline{w}_t^{(j)}}. \end{aligned}$$

The composite quasi log-likelihood function then becomes

$$\bar{l}(\theta) = \sum_{t=1}^{T-1} \left(-\frac{[p_{t+1} - \bar{\mu}(p_t)]^2}{2\bar{\sigma}^2(p_t)} - \frac{1}{2} \log [2\pi\bar{\sigma}^2(p_t)] \right),$$

and the corresponding composite quasi maximum likelihood estimator is given as $\bar{\theta} = \arg \max_{\theta} \bar{l}(\theta)$. In practice we choose the tuning parameters to be $n_i = 50,000$, $n_t = 32$ and $n_g = 128$, and therefore this routine is considerably more expensive than the above described simulated maximum likelihood routine, but still less costly than computing the full stationary distribution on the (x, z) -grid. As for the simulated maximum likelihood estimator, smoothness is barred by the interpolation required, and we therefore use the same Nelder-Mead type optimizer for maximizing $\bar{l}(\theta)$. Moreover, we rely on parametric bootstrap with (9-11) as data generating process for approximate standard errors.

Modulo Monte Carlo approximation error, it is seen that $\hat{\theta}$ maximizes $\sum_{t=2}^T \log \pi(p_t|p_1, \dots, p_{t-1})$, whereas $\bar{\theta}$ maximizes $\sum_{t=2}^T \log \pi(p_t|p_{t-1})$. A number of factors determine how much the two differ. In particular are $p_t|p_{t-1}$ and $p_t|p_1, \dots, p_{t-1}$ equal in distribution when the non-negativity constraint is binding, and therefore one would primarily expect the two estimators to differ when δ is small and stock-outs are infrequent.

Moreover, one would expect that the two would differ more at higher sampling frequencies or with values of ρ closer to 1 since then p_1, \dots, p_{t-2} are more informative with respect to p_t .

4 Simulation study

To study the performance of the proposed particle filter-based simulated ML estimator (SML) based on $\hat{l}(\theta)$, and also to compare with the composite ML (CML) estimator based on $\bar{l}(\theta)$, we conduct a simulation study. It should be noted that data are simulated using the numerical solution \hat{f} , and biases incurred by using \hat{f} instead of f in the estimation are consequently not visible in this study. See section 5.2 for a study of the sensitivity of parameter estimates to the grid size. Throughout, we use $N = 4096$ particles in the filter, and the real interest rate r is chosen to correspond to a 5% yearly rate. Each experiment is repeated 100 times and the true parameters in the data generating process (9-11) are taken to resemble those found in empirical applications. Throughout, the optimizations performed under SML and CML are started at the true parameters of the data generating process.

4.1 Monthly data experiment

In the first simulation study, we consider prices at an equivalent monthly frequency and true parameters inspired by natural gas real data. The bias, standard deviation and root mean square error (RMSE) are reported in Table 1 for different sample sizes $T = \{250, 500, 1000\}$. For the SML estimator, some biases are seen for the shorter sample size $T = 250$, but these biases seem to diminish for the larger sample sizes at a rate that is largely consistent with- or faster than what standard maximum likelihood theory would predict. Largely the same effects are seen for the standard deviations and RMSEs. Looking at the magnitudes of the RMSEs, we see that the parameters ρ and δ , which in large part determine the temporal dependence structure, are estimated with relatively good precision. On the other hand, a and b , which as a rule of thumb correspond to marginal location and scale of the price process sees relatively large RMSEs, in particular for the smaller sample sizes. This is related to the fact that the estimation of these parameters is strongly influenced by the price spikes, and the number and severity of price spikes vary substantially over the simulated data sets.

For CML, we obtain RMSEs that are consistently larger than those of SML, with differences being largest for a and b at the larger sample sizes. Moreover, in line with Michaelides and Ng (2000), substantial biases that vanishes only very slowly as T increases are seen for CML. Looking at relative computing times and errors induced by using Monte Carlo methods, we see that SML is substantially less expensive to evaluate and also produces consistently smaller Monte Carlo errors than those of CML.

		ρ	a	b	δ	(q-)log-like
True parameters		0.97	1.5	-0.4	0.02	
$T = 250, \tau_{SML} = 2.4s, \tau_{CML} = 7.1s$						
SML	Bias	-0.0146	-0.4821	-0.2173	0.0011	
	Std.dev.	0.0232	1.5897	0.9636	0.0078	
	RMSE	0.0273	1.6536	0.9831	0.0078	
	MC.Std.dev	0.0010	0.0315	0.0069	0.0007	0.0376
CML	Bias	-0.0264	-0.4200	-0.3923	0.0054	
	Std.dev.	0.0397	3.3513	1.3833	0.0086	
	RMSE	0.0475	3.3606	1.4311	0.0102	
	MC.Std.dev	0.0025	0.0841	0.0269	0.0005	0.0982
$T = 500, \tau_{SML} = 3.0s, \tau_{CML} = 11.8s$						
SML	Bias	-0.0050	-0.1110	-0.0340	0.0005	
	Std.dev.	0.0124	0.5020	0.2169	0.0050	
	RMSE	0.0133	0.5116	0.2185	0.0050	
	MC.Std.dev	0.0004	0.0095	0.0059	0.0002	0.0522
CML	Bias	-0.0185	-0.1922	-0.3953	0.0048	
	Std.dev.	0.0256	1.6313	0.8874	0.0071	
	RMSE	0.0315	1.6344	0.9673	0.0085	
	MC.Std.dev	0.0011	0.0195	0.0060	0.0005	0.0884
$T = 1000, \tau_{SML} = 3.9s, \tau_{CML} = 19.5s$						
SML	Bias	-0.0021	-0.0258	0.0028	0.0004	
	Std.dev.	0.0065	0.2280	0.0664	0.0031	
	RMSE	0.0068	0.2284	0.0661	0.0031	
	MC.Std.dev	0.0003	0.0084	0.0026	0.0002	0.0191
CML	Bias	-0.0109	-0.1408	-0.3801	0.0047	
	Std.dev.	0.0101	1.4722	0.7430	0.0054	
	RMSE	0.0149	1.4715	0.8313	0.0071	
	MC.Std.dev	0.0020	0.1067	0.0280	0.0007	0.0970

Note: True parameters indicated in the uppermost row and r corresponding to monthly data. Bias, statistical standard errors (Std.dev) and root mean squared errors (RMSE) are based on 100 replicas, with all replicas for SML converged. For CML, the number of failed and ignored replica were 1 ($T = 250$), 1 ($T = 500$) and 2 ($T = 1000$). For both SML and CML, different random number seeds were used in all replica, and $N = 4096$ particles were employed for SML. Monte Carlo Standard errors (MC.Std.dev) are calculated from 10 repeated estimations to a simulated data set with different random number seeds. τ_{SML} and τ_{CML} denote the mean (clock-)time of evaluating a (quasi-)log-likelihood function on a Dell Latitude E6510 laptop with an Intel Core i7 CPU 1.73 GHz CPU with 8 cores running Linux.

Table 1: Simulation study for the model (9-11), monthly data experiment.

4.2 Weekly data experiment

Our second simulation study involves prices at an equivalent weekly frequency and true parameters similar to those obtained for export prices from Norway on fresh farmed Atlantic Salmon³. The design of the experiment is otherwise equal to the monthly data experiment and the results are provided in Table 2. As in the previous experiment, SML appear to work satisfactory, with small biases for the larger sample sizes and RMSEs decaying as $T^{-1/2}$ or faster. In line with what was found for the monthly data experiment, it is seen that the temporal dependence parameters ρ and δ are estimated with good precision in all cases, whereas the location and scale parameters a and b require more data to be accurately determined.

CML has again mostly larger RMSEs than SML in all cases except for b in the $T = 250$ case, for which SML results are dominated by a single extreme replica. In particular we see a non-vanishing bias for a -parameter for CML that again mirrors what was found by Michaelides and Ng (2000). The differences in computing time and Monte Carlo standard errors are also consistent with the previous experiment, with both higher computational cost and higher Monte Carlo standard errors associated with CML. We therefore conclude that also in this setup, SML is the better overall estimator.

4.3 Yearly data experiment

Earlier applications of the storage model (Deaton and Laroque, 1995, 1996) have relied on a yearly period modeling and yearly data. This leads to smaller supply shock autocorrelation, and therefore provide a situation that is somewhat less in favor of SML. In the yearly data experiment we consider sample sizes of $T = 100, 200$ years of data and true dynamics equal to the parameters obtained by Deaton and Laroque (1996) for Tin using yearly data between 1900 and 1987. Otherwise the design of the experiment is equal to the monthly data experiment and results are presented in Table 3.

Also here it is seen that SML works very satisfactory with small biases throughout. Moreover, the Monte Carlo standard errors are substantially smaller than the statistical standard errors. In this situation, it is seen that the biases for CML vanishes faster than the monthly and weekly situations. Still for CML, we see larger biases and RMSEs than for SML. Taking into account that CML is more computationally costly than SML, we conclude that SML is the preferred estimator, even for data at a yearly frequency.

4.4 Effects of estimation bias on implied price characteristics

Table 4 investigates the effects of the estimation bias on implied price characteristics for the monthly, weekly and yearly data experiments. Using the true and “biased” parameters from the estimations in table 1 and 2,

³The real data used are between week 1, 1995 and week 39, 2012. The prices were normalized to mean 1. Prices can be found at <http://www.nosclearing.com/>

		ρ	a	b	δ	(q-)log-like
True Parameters		0.99	1.65	-0.09	0.0035	
$T = 250, \tau_{SML} = 2.5s, \tau_{CML} = 7.3s$						
SML	Bias	-0.0079	-0.1401	-0.1473	0.0004	
	Std.dev.	0.0294	0.3970	1.2646	0.0025	
	RMSE	0.0303	0.4191	1.2669	0.0026	
	MC.Std.dev	0.0002	0.0044	0.0008	2.8e-5	0.0096
CML	Bias	-0.0179	0.1668	-0.0966	0.0024	
	Std.dev.	0.0268	0.6931	0.1865	0.0033	
	RMSE	0.0321	0.7095	0.2092	0.0041	
	MC.Std.dev	0.0011	0.0428	0.0028	0.0004	0.1237
$T = 500, \tau_{SML} = 2.9s, \tau_{CML} = 12.1s$						
SML	Bias	-0.0021	-0.0024	-0.0107	0.0003	
	Std.dev.	0.0068	0.2189	0.0470	0.0013	
	RMSE	0.0071	0.2178	0.0480	0.0013	
	MC.Std.dev	0.0001	0.0010	0.0005	3.1e-5	0.0120
CML	Bias	-0.0174	0.2663	-0.1654	0.0025	
	Std.dev.	0.0562	0.5712	0.6448	0.0030	
	RMSE	0.0585	0.6277	0.6626	0.0039	
	MC.Std.dev	0.0046	0.2099	0.0168	0.0008	0.9993
$T = 1000, \tau_{SML} = 3.9s, \tau_{CML} = 19.9s$						
SML	Bias	-0.0006	-0.0083	-0.0015	-8.0e-7	
	Std.dev.	0.0023	0.1590	0.0123	0.0007	
	RMSE	0.0024	0.1584	0.0123	0.0007	
	MC.Std.dev	1.5e-5	0.0057	0.0002	1.3e-5	0.0325
CML	Bias	-0.0060	0.4690	-0.0754	0.0025	
	Std.dev.	0.0063	0.5164	0.1470	0.0023	
	RMSE	0.0087	0.6956	0.1646	0.0034	
	MC.Std.dev	0.0063	0.3497	0.0434	0.0004	0.5395

Note: True parameters indicated in the uppermost row and r corresponding to weekly data. Bias, statistical standard errors (Std.dev) and root mean squared errors (RMSE) are based on 100 replicas, with all replicas for SML converged. For both SML and CML, different random number seeds were used in all replica, and $N = 4096$ particles were employed for SML. Monte Carlo Standard errors (MC.Std.dev) are calculated from 10 repeated estimations to a simulated data set with different random number seeds. τ_{SML} and τ_{CML} denote the mean (clock-)time of evaluating a (quasi-)log-likelihood function on a Dell Latitude E6510 laptop with an Intel Core i7 CPU 1.73 GHz CPU with 8 cores running Linux.

Table 2: Simulation study for the model (9-11), weekly data experiment.

		ρ	a	b	δ	(q-)log-like
True Parameters		0.918	0.223	-0.038	0.046	
$T = 100, \tau_{SML} = 2.1s, \tau_{CML} = 4.0s$						
SML	Bias	-0.0047	0.0007	-0.0008	0.0054	
	Std.dev.	0.0338	0.0391	0.0063	0.0234	
	RMSE	0.0339	0.0389	0.0063	0.0238	
	MC.Std.dev	0.0003	0.0002	3.4e-5	0.0001	0.0117
CML	Bias	-0.0197	0.0258	-0.0200	-0.0040	
	Std.dev.	0.0338	0.0445	0.0122	0.0318	
	RMSE	0.0390	0.0512	0.0234	0.0319	
	MC.Std.dev	0.0021	0.0015	0.0012	0.0008	0.0469
$T = 200, \tau_{SML} = 2.3s, \tau_{CML} = 5.3s$						
SML	Bias	-0.0026	0.0008	-0.0011	-0.0020	
	Std.dev.	0.0219	0.0293	0.0044	0.0144	
	RMSE	0.0220	0.0292	0.0045	0.0145	
	MC.Std.dev	0.0002	0.0010	3.2e-5	0.0001	0.0447
CML	Bias	-0.0157	0.0252	-0.0181	-0.0091	
	Std.dev.	0.0257	0.0359	0.0071	0.0140	
	RMSE	0.0300	0.0437	0.0195	0.0166	
	MC.Std.dev	0.0006	0.0016	0.0002	0.0009	0.1350

Note: True parameters indicated in the uppermost row and r corresponding to yearly data. Bias, statistical standard errors (Std.dev) and root mean squared errors (RMSE) are based on 100 replicas, with all replicas for SML converged. For both SML and CML, different random number seeds were used in all replica, and $N = 4096$ particles were employed for SML. Monte Carlo Standard errors (MC.Std.dev) are calculated from 10 repeated estimations to a simulated data set with different random number seeds. τ_{SML} and τ_{CML} denote the mean time of evaluating a (quasi-)log-likelihood function on a 2016 imac with an 3.1 Ghz Intel Core i5. Only a single tread was used.

Table 3: Simulation study for the model (9-11), yearly data experiment.

	$E(p_t)$	$SD(p_t)$	$SK(p_t)$	$KU(p_t)$	$AC_1(p_t)$	P(stock out)
Monthly data experiment						
True dynamics	0.8583	0.6752	2.3978	10.6107	0.9677	0.0423
T=250, SML	0.6641	0.5045	3.2359	19.2188	0.9448	0.0298
T=500, SML	0.8047	0.6056	2.5399	11.8934	0.9608	0.0412
T=1000, SML	0.8517	0.6473	2.3629	10.4207	0.9653	0.0454
T=250, CML	0.7440	0.5582	3.2888	20.0495	0.9294	0.0359
T=500, CML	0.8396	0.6599	3.2027	18.5543	0.9397	0.0377
T=1000, CML	0.8423	0.7309	3.2759	18.7207	0.9492	0.0333
Weekly data experiment						
True dynamics	1.2018	0.4022	1.0890	4.3193	0.9909	0.0119
T=250, SML	1.0349	0.3683	1.8842	9.3327	0.9817	0.0132
T=500, SML	1.1989	0.3820	1.1783	4.6949	0.9887	0.0145
T=1000, SML	1.1992	0.3888	1.1095	4.4118	0.9902	0.0111
T=250, CML	1.3514	0.3570	1.4318	6.1169	0.9714	0.0261
T=500, CML	1.3727	0.4125	1.6494	7.4317	0.9716	0.0257
T=1000, CML	1.5070	0.5417	1.2826	4.9978	0.9848	0.0244
Yearly data experiment						
True dynamics	0.1922	0.0875	0.4582	2.8062	0.9063	0.0733
T=100, SML	0.1941	0.0871	0.4462	2.8027	0.8991	0.0846
T=200, SML	0.1913	0.0876	0.4826	2.8363	0.9050	0.0771
T=100, CML	0.1928	0.1058	0.8067	3.3511	0.8949	0.0688
T=200, CML	0.1921	0.1041	0.8074	3.3503	0.8997	0.0717

Note: All figures are calculated from one million periods of simulated dynamics. “True dynamics” are calculated from dynamics with parameters equal to those of the “True parameters” rows of Tables 1, 2 and 3. The remaining figures are calculated from dynamics with parameters equal to “True parameters” plus “Bias” taken from Tables 1, 2 and 3. SD denotes standard deviations, SK skewness, KU kurtosis, AC_1 first order autocorrelation and $P(\text{stock out})$ denotes the marginal probability of being in a stock-out state, i.e. $P(x_t) = f(x_t, z_t)$.

Table 4: The effect of estimation bias on price characteristics

we calculate and compare the mean, standard deviation, skewness, kurtosis and first order autocorrelation of model simulated prices. We also calculate the marginal probability a stock out as implied by the estimated models. This is done using both the monthly and weekly data experiment parameters. What is immediately clear from the table is that for the SML estimator, bias declines over all statistics as more price observations become available. This is not so for the CML estimator. For some of the statistics, for instance the mean in the weekly data experiment or the kurtosis in the monthly data experiment, the bias increases as more data becomes available. Overall the SML estimator displays favorable large sample properties and improved precision over the CML estimator. We also note that the CML estimator consistently underestimates the price autocorrelation. This is relevant as low implied price autocorrelation has been pointed to as a weakness of the competitive storage model (Deaton and Laroque, 1996; Cafiero et al., 2011).

4.5 Robustness to misspecification

A reason for opting for composite likelihood methods is that in many cases such methods may be more robust to model misspecification than methods based on the full likelihood. See e.g. Cox and Reid (2004) or Varin et al. (2011), section 4.3 for a detailed discussion of the robustness properties associated with composite likelihood. To compare CML and SML under misspecification, we carry out a Monte Carlo study where in the data generating process, η_t in (9) is taken to be a scaled t_4 -distribution with unit variance. The estimation methodology is left unchanged, and we consider the an identical setup as for the yearly data experiment discussed in Section 4.3.

The results are presented in Table 5. It is seen that the changes in performance under misspecification is relatively minor for both methods (i.e. relative to Table 3). In particular, we see that the relative performance between SML and CML is largely unchanged when misspecified η_t is added to the data generating process. Thus, at least for this situation and a heavy-tailed form of misspecification, the benefits from employing the potentially more robust CML are too small to outweigh the statistical accuracy stemming from using a full likelihood specification as in SML.

5 Empirical Application

To illustrate our estimation procedure with real data we apply it to monthly frequency observations on natural gas spot prices. To compare model fit and precision of parameter estimates we apply both our filter-based estimator and the composite likelihood estimator. One way to empirically asses the relevance of speculative storage model is to compare the storage model fit to a benchmark linear AR(1) model. It is straightforward to show that zero storage (which might occur if the cost of storage is sufficiently large) in the storage model

		ρ	a	b	δ
True parameters		0.918	0.223	-0.038	0.046
$T = 100, \tau_{SML} = 2.1s, \tau_{CML} = 4.0s$					
SML	Bias	-0.0095	0.0041	-0.0017	-0.0029
	Std.dev.	0.0375	0.0355	0.0085	0.0206
	RMSE	0.0385	0.0356	0.0086	0.0207
CML	Bias	-0.0362	0.0237	-0.0220	-0.0072
	Std.dev.	0.0442	0.0427	0.0186	0.0284
	RMSE	0.0570	0.0487	0.0288	0.0292
$T = 200, \tau_{SML} = 2.3s, \tau_{CML} = 5.3s$					
SML	Bias	0.0005	0.0015	0.0005	-0.0049
	Std.dev.	0.0207	0.0265	0.0048	0.0142
	RMSE	0.0206	0.0265	0.0048	0.0149
CML	Bias	-0.0218	0.0218	-0.0170	-0.0034
	Std.dev.	0.0333	0.0328	0.0127	0.0201
	RMSE	0.0396	0.0392	0.0212	0.0203

Note: True parameters indicated in the uppermost row and r corresponding to yearly data. Bias, statistical standard errors (Std.dev) and root mean squared errors (RMSE) are based on 100 replicas, with all replicas for SML converged. For both SML and CML, different random number seeds were used in all replica, and $N = 4096$ particles were employed for SML. τ_{SML} and τ_{CML} denote the mean time of evaluating a (quasi-)log-likelihood function on a 2016 imac with an 3.1 Ghz Intel Core i5. Only a single tread was used.

Table 5: Simulation study for the model (9-11) subject to misspecification in η_t .

implies that prices evolve as

$$p_{t+1} = a + \rho(p_t - a) + b\epsilon_{t+1}, \epsilon_t \sim \text{i.i.d. } N(0, 1). \quad (16)$$

Rejecting the linear AR(1) model in favor of the storage model does not imply that the storage model is the “true” model, but provides support for characteristics consistent with speculative storage over a model where prices are explained by a linear first order process. One reason why a linear AR(1) model might be rejected in favor of the storage model is stochastic volatility in the data. To investigate stochastic volatility we also estimate the linear AR(1) model with GARCH(1,1) errors. Finally, given the storage model predicts a two-state regime switching type price dynamics, we estimate a Markov switching (MS) model, where the AR(1) model in equation 16 is allowed to change between two regimes as determined by a latent two-state Markov process with constant transition probabilities.

Comparing the fit of the competitive storage model to reduced form time-series models is a strong test. The reduced form models (such as the linear AR(1) model or the GARCH models) are specifically designed to account for specific features of the data (such as first-order autocorrelation or ARCH effects). The value of such a comparison is that we can identify price features that the model is able to account for, and where improvements are needed. Finally, we note that all models considered are estimated using commodity price

data only.

5.1 Application to Natural Gas at Henry Hub

The natural gas price in this analysis is the spot price at the Henry Hub terminal in Louisiana. Prices are denoted in US\$ per thousand cubic meters of gas, and covers the period 1991 M1 to 2012 M6. Prices can be obtained from <http://www.imf.org/external/np/res/commod/index.aspx>. Natural gas prices are influenced by a range of factors such as the price of oil, weather, seasonality in demand, shut-in production and storage (Brown and Yucel, 2008). In regards to storage, inventories play an important role in smoothing production and balancing demand–supply conditions. The release of information on inventory levels is known to generate considerable volatility in prices (Mu, 2007). Chiou Wei and Zhu (2006) further demonstrate that the convenience yield (measured as the difference between the spot and forward natural gas price) is negatively related to natural gas inventory levels. This suggests that abnormally high prices are related to low inventories, as implied by the storage model.

The storage model is arguably too simple to capture the full complexities of the real market. Effects related to energy substitution (the oil price effect) and seasonality in demand is not specifically modeled, and is likely captured by the supply shocks. However, if speculative storage effects are present to any substantial degree, inference should favor the storage model over the linear AR(1) model (equation 16). An added benefit of analyzing the natural gas market is that detailed information on natural gas storage is available. This means we can compare the model implied filtered storage, derived using only the price data, to actual storage levels. A strong correspondence between these series will provide support for the relevance of the storage model and the estimation procedure.

Prior to estimation the price data was normalized to unit mean. Parameter estimates are provided in Table 6. We see that SML and CML produce similar results, but that SML has smaller Monte Carlo standard errors. The statistical- and Monte Carlo standard error for the real data are largely consistent with those found in the simulation study reported in Table 1, $T = 250$. Compared to the AR(1) benchmark, the storage model performs substantially better in terms of model fit. This implies that not all of the model fit comes from the exogenous latent AR(1) shock; the economic model appears relevant in terms of explaining observed characteristics.

Adding GARCH(1,1) errors to the AR(1) model gives an improved fit with a log-likelihood of 148.79, where the AR(1)-GARCH(1,1) model has one more parameter than the storage model. However, the log-likelihood is still below the fit of the storage model. Due to the non-nested nature of the AR(1)-GARCH(1,1) model and the storage model (9-11), we also computed the log-likelihood ratios of the storage model against

	ρ	a	b	δ	log-likelihood	
SML						
Estimate	0.968	1.471	-0.408	0.0212	194.32	
MC Std.Dev	2.9e-5	4.2e-4	1.8e-4	1.0e-5	4.6e-3	
Statistical S.E.	0.0265	1.457	0.489	0.0083		
CML						
Estimate	0.963	2.075	-0.599	0.0275	192.19	
MC Std.Dev	0.0039	0.237	0.0759	0.0016	0.288	
Statistical S.E.	0.0465	1.213	1.360	0.0102		
Benchmark AR(1) model (16)						
Estimate	0.950	1.021	-0.188		65.34	
Statistical S.E.	0.0192	0.625	0.0083			
Markov-Switching AR(1) model, $P(\text{Regime 1 next period} \text{Regime 1 current period})=0.951,$ $P(\text{Regime 1 next period} \text{Regime 2 current period})=0.081$						
Estimate (Regime 1)	0.887	0.549	-0.064		164.09	
Statistical S.E. (Regime 1)	0.0164	0.014	0.0048			
Estimate (Regime 2)	0.861	1.725	-0.28			
Statistical S.E. (Regime 2)	0.0492	0.884	0.022			
AR(1)-GARCH(1,1) (cond. variance model: $\sigma_t^2 = \alpha_0 + \alpha_1 \epsilon_{t-1}^2 + \beta_1 \sigma_{t-1}^2$)						
	ρ	a	α_0	α_1	β_1	
Estimate	0.967	0.520	4.1e-4	0.046	0.667	148.79
Statistical S.E.	0.0155	0.396	2.5e-4	0.095	0.044	

Note: Standard errors are based on 100 parametric bootstrap replicas, and MC standard errors are based on fitting the model to the real data 30 times with different random number seeds in the particle filter. The benchmark AR(1) model was fitted using maximum likelihood, and statistical standard errors are based on observed Fisher information.

Table 6: Parameter estimates for the natural gas data.

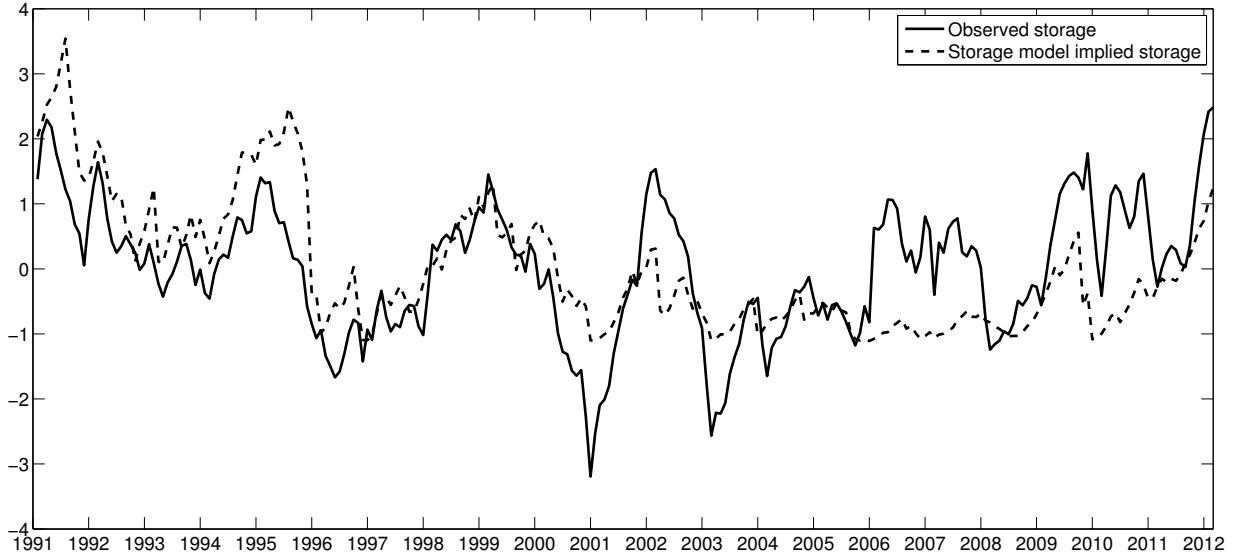
the AR(1)-GARCH(1,1) model for the 100 parametric bootstrap replica reported in Table 6 ⁴. We find that the observed log-likelihood ratio ($2(194.32 - 148.79) = 91.06$) fall between the 61st and 62nd simulated likelihood ratio when the storage model is the true model, which indicate that the observed log-likelihood ratio is consistent with the storage model being the “true” model.

The MS-AR(1) produces a fit with log-likelihood of 164.09, which is again substantially below the structural model while containing four more parameters. To assess this number, we fitted the MS-AR(1) model to the simulated data under the storage model as described above. We find that the observed likelihood ratio ($2(194.32 - 163.02) = 60.46$) fall between the 13th and 14th simulated likelihood ratio when the storage model is the true model, which is again consistent with the storage model being the better model.

Finally, we fitted model (9-11) with iid supply shock (i.e. $\rho = 0$) to compare with a methodology similar to that of Cafiero et al. (2011). We used the same price function solver and conditionally Gaussian transition densities for the price process so that the iid supply shock model is nested under the general model (9-11). We obtain a log-likelihood of 190.79 for the iid supply shock model, which correspond to a rejection of the iid model against the general storage model (9-11) with p -value 0.008. It is also worth noticing that the fitted price function has a very large negative $b = -189$, and therefore we regard this model fit as nonsensical.

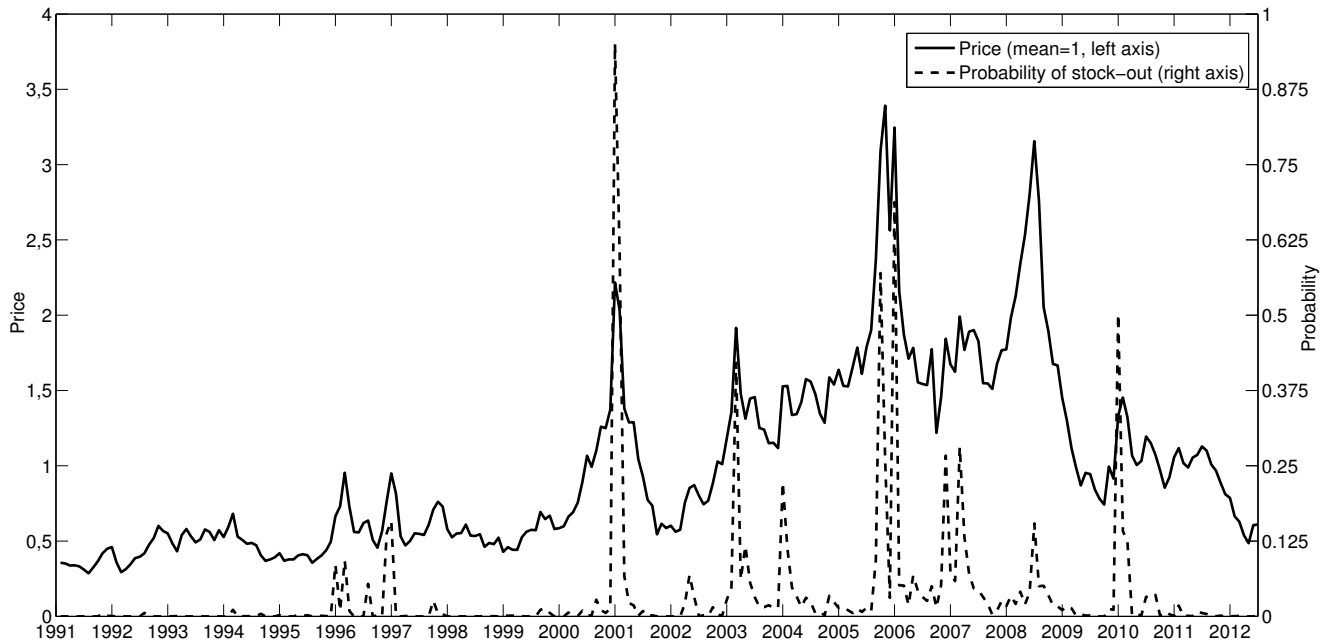
Figure 1 plots the deseasonalized and detrended observed monthly storage of natural gas against the median model implied storage. Considering that inference on model storage only uses price data, the two series’ are similar. There is good correspondence between the series’, especially up to the early 2000’s. In later years, the variation in storage is larger than what is predicted by the storage model. The relatively strong similarity between the series’ is reassuring as it suggests that the latent model storage is related to actual storage. The figure gives support for the relevance of the storage model and the importance of inventories in accounting for natural gas price movements.

Finally, to explore the effect of the non-negativity constraint on price dynamics we plot the price series (unit mean) and the filtered model implied probability of a stock-out. This is shown in Figure 2. The probability of a stock-out is the probability that the next period stock falls below a level where any positive speculative storage is optimal. The constraint is the source of non-linearity in the model, and as the figure shows the constraint is likely to be binding in certain periods. These are periods associated with abnormally high prices. Looking at the storage data in Figure 1 we observe that periods with higher probability of a stock-out coincide with periods of low storage. The figure highlights the importance and relevance of the non-negativity constraint in accounting for characteristics in the price data.



Note: Observed storage is the deseasonalized and detrended U.S. Natural Gas Underground Storage Volume (MMcf) (<http://www.eia.gov/naturalgas/>). The series is deseasonalized using trigonometric functions with annual frequency. A linear trend is used for detrending. All series' are normalized to have mean zero and unit standard deviation.

Figure 1: Observed and model implied storage.



Note: The filtered probabilities of stock-out at time t are calculated as $Prob(f(x_t, z_t) = P(x_t) | p_1, \dots, p_t)$ using particle filter output.

Figure 2: Natural gas price and model suggested probability of stock-out

	Natural gas data		
	Data	Storage model	AR(1)
$E(p_t)$	1	0.86	1.02
$SD(p_t)$	0.61	0.67	0.61
$SK(p_t)$	1.29	2.26	-0.05
$EKU(p_t)$	1.68	6.46	0.03
$AC_1(p_t)$	0.95	0.96	0.95
$AC_2(p_t)$	0.90	0.94	0.90
$AC_1(\Delta p_t)$	0.47	0.40	0.00

Note: The statistics for the estimated models are calculated over simulated realizations of length 100,000. SD denotes standard deviations, SK skewness, EKU excess kurtosis, AC_k the k -th order autocorrelation and in particular $AC_1(|\Delta p_t|)$ denotes the first order autocorrelation of the absolute price returns as a measure of volatility clustering.

Table 7: Comparison of statistics from data and estimated models.

	Residuals from Natural Gas Data	
	storage model	AR(1) model
Mean	0.0175	-0.0001
Standard Deviation	0.9742	1.0001
Skewness	0.5999	-0.2546
Excess Kurtosis	0.5668	7.2735
First Order Autocorrelation	0.1877	0.0252
Jarque-Bera p -value	0.0026	<0.0010
Kolmogorv-Smirnoff p -value	0.3493	<0.0001
Ljung-Box test (lag=20) p -value	0.0014	0.0143
Engle ARCH test p -value	0.7648	<0.0001

Note: The residuals for the storage model are calculated by a standard Gaussian quantile transform applied to the generalized residuals (13). We expect that the residuals are approximately iid standard Gaussian if the model specification is correct.

Table 8: Diagnostics for residuals of the real data set.

5.2 Diagnostics

As a first set of diagnostics, we report in table 7 several statistics of the actual natural gas price along with the corresponding statistics for long realizations of the fitted storage and linear AR(1) models. It is seen that the AR(1) model captures better the mean, standard deviation and autocorrelation of the price series, whereas the storage model does a better job at capturing skewness, excess kurtosis and the autocorrelation of absolute price returns. The latter is used as a measure of volatility clustering, and it is seen that the storage model matches the data rather well in this sense. The large standard deviation of the storage model for the salmon data stems from the fact that this model produces infrequent price spikes that are substantially larger than what is seen in the data.

As a further diagnostic of model fits, we perform a battery of tests on the residuals. The results are given in Table 8. This diagnostics also helps highlight what features of the data the storage model addresses. Again,

⁴I.e. (9-11) with parameters found for SML is the data-generating process.

$M_{x,1}$	$M_{x,2}$	M_z	ρ	a	b	δ	log-likelihood
256	256	128	0.9670	1.5257	-0.4028	0.0217	194.2100
128	128	128	0.9672	1.5106	-0.4103	0.0217	194.3057
256	256	64	0.9671	1.4781	-0.3994	0.0211	194.2546
128	128	64	0.9666	1.4819	-0.4003	0.0217	194.3273

Note: The figures in the table were obtained by estimating the parameters using the real data sets. The random number seed was kept fixed, and it is seen that errors associated with price function solver discretization are small relative to the statistical standard deviations.

Table 9: Maximum likelihood estimates and optimal log-likelihoods for different resolutions of the rational expectation solver grids for the real data.

it is seen that the storage model in general does a better job accounting for higher moment characteristics. The storage model predicts non-linear first-order Markov prices. These features will manifest in the higher moments of prices, and it is not surprising that these are the characteristics the storage model best describes. Not surprising, the AR(1) benchmark does a better job when it comes to the unconditional mean price and first order autocorrelation, while the storage model does better in terms of excess kurtosis. In addition, the storage model better accounts for ARCH effects. In terms of the Gaussian structure of our parametric specification (equations (9-11)), the diagnostic results indicate that residuals are close to normal.

To assess whether we are using a sufficiently fine grid, we estimate the model on the natural gas and salmon data using different values of $M_{x,1}$, $M_{x,2}$ and M_z . As was demonstrated by (Cafero et al., 2011) under the $\rho = 0$ model, using too coarse grids can bias parameter estimates. Parameter estimates obtained while keeping the random number seed in the particle filter fixed are provided in Table 9. The settings of the lowermost rows in each panel of the table are the ones used for the above estimation on natural gas and salmon prices. For the natural gas data, differences in parameter estimates for finer grids are minor comparing to statistical standard errors from the SML panel in Table 6. All in all we conclude that we are using sufficiently fine grids for these ranges of parameters.

6 Conclusion

We propose a particle filter estimator for the competitive storage model with temporal supply shock dependence when only price data is available for estimation. The particle filter estimator utilizes information in the conditional distribution of prices when temporal dependence is present in the shocks. This is contrary to the composite pseudo maximum likelihood estimator of Deaton and Laroque (1995, 1996), which only utilizes the marginal state distribution to arrive at predictive price moments. To our knowledge this is the first attempt at using particle filter methods to estimate the competitive storage model. Our results suggest that the relative simplicity and low-dimensional nature of the partial equilibrium storage model makes it particularly suitable for particle filter estimators.

We demonstrate through simulation experiments that our particle filter estimator does a better job in terms of both the bias and precision of the structural parameter estimates compared to the composite estimator. Furthermore, our estimator is less computationally demanding than our Monte Carlo based implementation of the Deaton and Laroque composite maximum likelihood estimator, and also is more numerically stable. In addition, simulation evidence indicates that our model has favorable large sample properties where bias diminishes when more price data becomes available. The composite maximum likelihood estimator does not display this same general reduction in bias as sample size increases.

As an application and demonstration of the estimator we estimate the storage model to natural gas prices. As a benchmark, we compare the storage model to a linear AR(1) model, a GARCH(1,1) model and a two-state Markov Switching AR(1) model. The linear AR(1) model can be thought of as the price representation that would occur with zero speculative storage in the storage model. The comparison to reduced form models allows us to identify what features of prices the storage model is able to account for, and where improvements are needed. For the natural gas market, the storage model performs better than all reduced form time-series models considered. This suggests that the non-linearity in the model, arising from the non-negativity constraint on storage, is relevant to account for natural gas price characteristics. As support for the relevance of the storage model in the natural gas market, we find relatively strong correspondence between observed and model implied storage. Diagnostics show that the storage model addresses features in the higher moments of prices, specifically linked to excess kurtosis and ARCH effects.

The particle filter estimator appears superior to the composite maximum likelihood estimator for the type of model setting analyzed in this paper. The storage model is used to investigate effects of various commodity market policies. The value of such policy evaluations depend crucially on the validity of the structural parameters chosen for the analysis. When price data is the only reliable data available to infer structural parameters, and shocks are suspected to have temporal dependence, the particle filter estimator should be applied to efficiently utilize the sparse data.

References

- Andrieu, C., A. Doucet, and R. Holenstein (2010). Particle Markov chain Monte Carlo methods. *Journal of the Royal Statistical Society: Series B (Statistical Methodology)* 72(3), 269–342.
- Arseneau, D. M. and S. Leduc (2013). Commodity price movements in a general equilibrium model of storage. *IMF Economic Review* 61(1), 199–224.
- Aruoba, S. B., J. Fernandez-Villaverde, and J. F. Rubio-Ramirez (2006). Comparing solution methods for dynamic equilibrium economies. *Journal of Economic Dynamics and Control* 30(12), 2477 – 2508.
- Brennan, D. (2003). Price dynamics in the Bangladesh rice market: implications for public intervention. *Agricultural Economics* 29(1), 15–25.
- Brown, S. and M. Yucel (2008). What drives natural gas prices? *Energy Journal* 29(2), 45.

- Cafiero, C., E. Bobenrieth H., J. Bobenrieth H., and B. Wright (2011). The empirical relevance of the competitive storage model. *Journal of Econometrics* 162(1), 44–54.
- Cafiero, C., E. S. Bobenrieth H., J. R. Bobenrieth H., and B. D. Wright (2015). Maximum likelihood estimation of the standard commodity storage model: Evidence from sugar prices. *American Journal of Agricultural Economics* 97(1), 122–136.
- Cafiero, C., B. Wright, A. Sarris, D. Hallam, et al. (2006). Is the storage model a closed empirical issue? the empirical ability of the storage model to explain price dynamics. *Agricultural Commodity Markets and Trade. New Approaches to Analyzing Market Structure and Instability* 162, 89–114.
- Cappe, O., S. Godsill, and E. Moulines (2007). An overview of existing methods and recent advances in sequential monte carlo. *Proceedings of the IEEE* 95(5), 899–924.
- Chambers, M. J. and R. E. Bailey (1996). A theory of commodity price fluctuations. *Journal of Political Economy* 104(5), 924–957.
- Chiou Wei, S. and Z. Zhu (2006). Commodity convenience yield and risk premium determination: The case of the us natural gas market. *Energy Economics* 28(4), 523–534.
- Cox, D. R. and N. Reid (2004). A note on pseudolikelihood constructed from marginal densities. *Biometrika* 91(3), 729.
- Deaton, A. and G. Laroque (1992). On the behaviour of commodity prices. *The Review of Economic Studies* 59(1), 1–23.
- Deaton, A. and G. Laroque (1995). Estimating a nonlinear rational expectations commodity price model with unobservable state variables. *Journal of Applied Econometrics* 10, S9–S40.
- Deaton, A. and G. Laroque (1996). Competitive storage and commodity price dynamics. *The Journal of Political Economy* 104(5), 896–923.
- DeJong, D. N., R. Liesenfeld, G. V. Moura, J.-F. Richard, and H. Dharmarajan (2013). Efficient likelihood evaluation of state-space representations. *The Review of Economic Studies* 80(2), 538–567.
- Durbin, J. and S. J. Koopman (1997). Monte Carlo maximum likelihood estimation for non-Gaussian state space models. *Biometrika* 84(3), 669–684.
- Durham, G. B. (2006). Monte Carlo methods for estimating, smoothing, and filtering one and two-factor stochastic volatility models. *Journal of Econometrics* 133, 273–305.
- Eraker, B. (2001). MCMC analysis of diffusion models with application to finance. *Journal of Business and Economic Statistics* 19, 177–191.
- Fernandez-Villaverde, J. and J. F. Rubio-Ramirez (2007). Estimating macroeconomic models: A likelihood approach. *Review of Economic Studies* 74(4), 1059–1087.
- Funke, N., Y. Miao, and W. Wu (2011). Reviving the competitive storage model: A holistic approach to food commodity prices. IMF Working Papers 11/64.
- Geman, H. and W. O. Smith (2013). Theory of storage, inventory and volatility in the LME base metals. *Resources Policy* 38(1), 18–28.
- Gordon, N., D. Salmond, and A. Smith (1993). Novel approach to nonlinear/non-Gaussian Bayesian state estimation. *Radar and Signal Processing, IEE Proceedings F* 140(2), 107–113.
- Gouel, C. (2013a). Comparing numerical methods for solving the competitive storage model. *Computational Economics* 41(2), 267–295.
- Gouel, C. (2013b). Optimal food price stabilisation policy. *European Economic Review* 57, 118–134.

- Gourieroux, C., A. Monfort, and A. Trognon (1984). Pseudo maximum likelihood methods: Theory. *Econometrica* 52(3), pp. 681–700.
- Kaldor, N. (1939). Speculation and economic stability. *The Review of Economic Studies* 7(1), pp. 1–27.
- Kleppe, T. S. and H. J. Skaug (2016). Bandwidth selection in pre-smoothed particle filters. *Statistics and Computing* 26(5), 1009–1024.
- Liesenfeld, R. and J.-F. Richard (2003). Univariate and multivariate stochastic volatility models: estimation and diagnostics. *Journal of Empirical Finance* 10, 505–531.
- Lindsay, B. G. (1988). Composite likelihood methods. *Contemporary Mathematics* 80, 221–239.
- Malik, S. and M. K. Pitt (2011). Particle filters for continuous likelihood evaluation and maximisation. *Journal of Econometrics* 165(2), 190 – 209.
- Michaelides, A. and S. Ng (2000). Estimating the rational expectations model of speculative storage: a Monte Carlo comparison of three simulation estimators. *Journal of Econometrics* 96, 231–66.
- Miranda, M. (1997). Numerical strategies for solving the nonlinear rational expectations commodity market model. *Computational Economics* 11(1-2), 71–87.
- Miranda, M. J. and J. W. Glauber (1993). Estimation of dynamic nonlinear rational expectations models of primary commodity markets with private and government stockholding. *The Review of Economics and Statistics* 75(3), 463–470.
- Miranda, M. J. and P. G. Helmerger (1988). The effects of commodity price stabilization programs. *American Economic Review* 78(1), 46–58.
- Miranda, M. J. and X. Rui (1996). An empirical reassessment of the commodity storage model. Technical report, Mimeo, Department of Agricultural Economics, Ohio State University.
- Mitraille, S. and H. Thille (2009). Monopoly behaviour with speculative storage. *Journal of Economic Dynamics and Control* 33(7), 1451–1468.
- Mu, X. (2007). Weather, storage, and natural gas price dynamics: Fundamentals and volatility. *Energy Economics* 29(1), 46–63.
- Ng, S. (1996). Looking for evidence of speculative stockholdings in commodity markets. *Journal of Economic Dynamics and Control* 20(1-3), 123–43.
- Ng, S. and F. J. Ruge-Murcia (2000). Explaining the persistence of commodity prices. *Computational Economics* 16(1-2), 149–171.
- Osborne, T. (2004). Market news in commodity price theory: Application to the Ethiopian grain market. *The Review of Economic Studies* 71(1), 133–164.
- Pitt, M. K., R. dos Santos Silva, P. Giordani, and R. Kohn (2012). On some properties of Markov chain Monte Carlo simulation methods based on the particle filter. *Journal of Econometrics* 171(2), 134 – 151.
- Richard, J.-F. and W. Zhang (2007). Efficient high-dimensional importance sampling. *Journal of Econometrics* 127(2), 1385–1411.
- Shephard, N. and M. K. Pitt (1997). Likelihood analysis of non-Gaussian measurement time series. *Biometrika* 84, 653–667.
- Silvermann, B. W. (1986). *Density Estimation for Statistics and Data Analysis*. New York: Chapman and Hall.
- Tauchen, G. (1986). Finite state Markov-chain approximations to univariate and vector autoregressions. *Economics Letters* 20(2), 177 – 181.

- Varin, C., N. Reid, and D. Firth (2011). An overview of composite likelihood methods. *Statistica Sinica* 21(1), 5–42.
- Varin, C. and P. Vidoni (2008). Pairwise likelihood inference for general state space models. *Econometric Reviews* 28(1-3), 170–185.
- Williams, J. B. (1936). Speculation and the carryover. *The Quarterly Journal of Economics* 50(3), 436–455.
- Working, H. (1949). The theory of the price of storage. *American Economic Review* 39, 1254–1262.
- Wright, B. and J. Williams (1982). The economic role of commodity storage. *The Economic Journal* 92, 596–614.

A Fourier transform-based continuous resampling routine

Suppose we wish to sample from a univariate Gaussian mixture on the form

$$\pi(z) = \sum_{j=1}^N w^{(j)} \mathcal{N}(z | \mu^{(j)}, \sigma^2).$$

Then the practical fast Fourier transform routine consist of the following steps:

- Grid: Find the mean and standard deviation of $\pi(z)$ and initiate a n_g -point regular grid containing say the mean ± 8 standard deviations. We set n_g to 1024 in all computations presented in this paper.
- PDF: As the variance in each component of $\pi(z)$ is equal, the PDF may be computed using fast Fourier transform methods on the regular grid as explained thoroughly in Silvermann (1986), section 3.5 (with the modification that each particle weight is now $w^{(j)}$ and not $1/n$).
- CDF: Compute the cumulative distribution function (CDF) of the approximate probability density function on the same grid using a mid-point rule for each grid point.
- Fast inversion: Sample approximate random variables from $\pi(z)$ based on stratified uniforms using the CDF-inversion algorithm provided in Appendix A.3 of Malik and Pitt (2011).

The total operation count of this algorithm is $O(N + n_g \log_2(n_g))$ and thus is it linear in complexity in the number of particles retained also for this form of continuous sampling with fixed n_g . However, it is worth noticing that to obtain the asymptotically correct random draws (i.e. exact quantiles corresponding to the stratified uniform random numbers) as $N \rightarrow \infty$, n_g must also grow, e.g. as $O(N)$. Moreover, the area covered by the grid must also grow, but at a slower rate, e.g. $O(\log(N))$.